Vacuum polarization in a strong Coulomb field. III. Nuclear size effects*

Lowell S. Brown, Robert N. Cahn, and Larry D. McLerran
Physics Department, University of Washington, Seattle, Washington 98195
(Received 6 March 1975)

We compute the change in the vacuum polarization near a high-Z nucleus arising from the finite extent of the nuclear charge density. A massless-electron technique is exploited to permit an analytical calculation of the effect to all orders in $Z\alpha$. Applications to muonic atoms are of particular interest as tests of quantum electrodynamics. The calculation of muonic energy level shifts is carried out to lowest order in the ratio of the nuclear radius to the radius of the muonic orbit. This approximation is appropriate to many muonic states with large orbits. Our analytical results are in excellent agreement with numerical studies by Gyulassy and give as a special case the order $\alpha(Z\alpha)^3$ calculation of Arafune. The effect on muonic x rays such as those produced in the $5g_{9/2} \rightarrow 4f_{7/2}$ transition in ^{208}Pb is about 5 eV, increasing slightly the discrepancy between theory and experiment in such systems.

I. INTRODUCTION

Quantum electrodynamics predicts deviations from pure Coulombic behavior near a point charge. The potential energy of a charge $-e$ located a distance r from a charge $+Ze$ is modified from $V_{\text{Coul}}(r) = -Z\alpha/r$ by the vacuum-polarization charge density which extends out to a distance of roughly half the Compton wavelength of the electron, $\lambda\!\!\!^{-}_e/2$. The term in the vacuum polarization of order $\alpha Z\alpha$, represented in Fig. 1(a), is called the Uehling term[1]; after an infinite charge renormalization it yields a correction to V_{Coul} given by

$$V_{\text{Ueh}}(r) = -\frac{\alpha Z\alpha}{\pi r}\int_{2m_e}^{\infty} d\kappa\, e^{-\kappa r}\left(\frac{2}{3\kappa^2}+\frac{4m_e^2}{3\kappa^4}\right) \times (\kappa^2 - 4m_e^2)^{1/2}. \quad (1)$$

For large values of Z, the vacuum polarization in orders $\alpha(Z\alpha)^n$, $n = 3, 5, 7\ldots$ must be considered as well. These terms, represented in Fig. 1(b), have been discussed extensively by Wichmann and Kroll.[2] In an earlier paper,[3] we verified a central result of Wichmann and Kroll: the value of the induced vacuum-polarization point charge, $\delta Q'$, in orders $\alpha(Z\alpha)^n$, $n = 3, 5, 7, \ldots$. We have also extended the results of Wichmann and Kroll by calculating the short-distance behavior of the vacuum-polarization charge density near a point nucleus.[4]

These corrections to Coulomb's law caused by the vacuum polarization at small distances are of great interest because they can be measured quite accurately by x-ray transitions in muonic atoms. Muons captured into atomic orbits cascade down through electric dipole radiation and by the time they reach low values of the principal quantum number, populate preferentially circular orbits. The radius of such an orbit is $a_\mu = n^2/(Z\alpha m_\mu)$, which is, for several values of the principal quantum number n, much smaller than the first electronic radius $[a_e = 1/(Z\alpha m_e)]$ and the dimension of the vacuum-polarization cloud $[\lambda\!\!\!^{-}_e/2]$. Except for the very first values of n, the circular orbits stay well outside the nucleus. In these circumstances the muon provides a sensitive measure of the vacuum-polarization effects, unobscured by the complexities of nuclear physics.

Both the Uehling result and the Wichmann-Kroll result for the induced point charge have been substantially verified in such muonic x-ray experiments. However, when many small, calculable effects such as electron screening and the Lamb shift are included, there still remains a discrepancy between the theoretical predictions and the

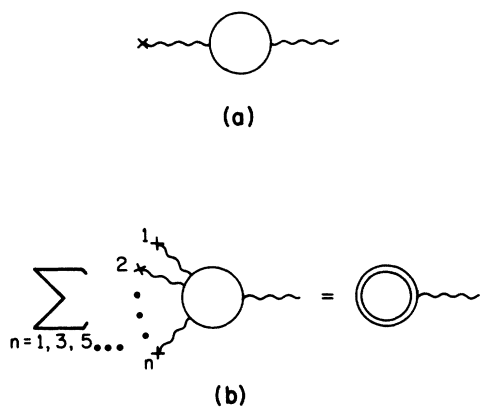

FIG. 1. (a) A representation of the Uehling potential. The nucleus is represented by $\times$. (b) A representation of all vacuum-polarization effects of order $\alpha(Z\alpha)^n$, $n = 1, 3, 5, \ldots$. If $\times$ represents a point source, the potential is the one discussed in Refs. 2–4. The present calculation corresponds to the difference between having $\times$ represent a point source and having it represent a nucleus of finite extent.

experimental data for a number of transitions[5,6] including $5g_{9/2} \to 4f_{7/2}$ in ^{208}Pb.

A possible source of the discrepancy is the finite extent of the nuclear charge distribution.[7-10] By Gauss's law, a muon remaining outside the nucleus is not affected directly by the details of a spherically symmetric charge distribution inside. However, the vacuum-polarization virtual electrons and positrons which penetrate the nucleus are influenced by the nuclear charge distribution. The resulting distortion of the vacuum-polarization cloud extends out to the Bohr radius of the orbiting muons and shifts their energy levels.

Since the vacuum polarization leaves the total charge of the nucleus unchanged, the potential at a distance r from the nucleus can be determined once the vacuum-polarization charge density is known at radii greater than r: The charge inside r is simply the negative of the charge outside r, and contributes in a Coulomb-type fashion to the potential. Thus it suffices to expand the vacuum-polarization charge density in the ratio of the nuclear radius to r, since we shall be concerned only with values of $r \gtrsim a_\mu$, which is itself much larger than the nuclear radius for the cases of interest to us.

Motivated by the large value of $\lambda\!\!\!^{-}_e$ relative to other length scales in the problem, we shall set the mass of the electron to zero. Evidence for the appropriateness of this approximation is given below. It is essential to our techniques, which then permit an analytical calculation to all orders in $Z\alpha$.

The details of the nuclear charge distribution enter our calculation through a single quantity, G/F, the ratio of the small to the large components of the solution to the Dirac equation about the nuclear charge distribution. The relevant solution here is the one regular at the origin, evaluated at the nuclear surface, for an electron of zero energy and mass. Thus G/F can be obtained by simple numerical integration using the measured nuclear charge distribution.

In practice, we find it convenient to use a model electrostatic potential inside the nucleus:

$$V(r) = A(r^2 + a^2)^{-1/2}. \tag{2}$$

This potential is joined continuously to a pure Coulomb field outside the nucleus. In Fig. 2 the model potential with suitable values of the parameters is compared to the potential derived from the measured charge distribution for ^{208}Pb.

Our result for the modification of the vacuum-polarization potential energy due to the finite nuclear size is[9]

$$\delta V(r) = \frac{\alpha}{\pi r}\left(\frac{b}{r}\right)^{2\lambda}\left[\frac{G/F - Z\alpha/(1+\lambda)}{1-[Z\alpha/(1+\lambda)](G/F)}\right]\frac{\Gamma(4\lambda)}{\lambda^2(2\lambda+1)^2} \times \left|\frac{\Gamma(\lambda + iZ\alpha)}{\Gamma(2\lambda)}\right|^4, \tag{3}$$

where b is the nuclear radius and $\lambda = [1-(Z\alpha)^2]^{1/2}$. The result is completely general and has no model dependence. If the finite-size correction were required only for the $\alpha Z\alpha$ term, Eq. (1) could be integrated over the nuclear charge density, with the result[5,11]

$$\delta V_{\text{Ueh}}(r) = \frac{\alpha Z\alpha}{\pi}\left\{-\frac{1}{9}\frac{\langle r^2\rangle_{\text{nuc}}}{r^3} + \frac{1}{3}\frac{m_e^2\langle r^2\rangle_{\text{nuc}}}{r} - \frac{1}{30}\frac{\langle r^4\rangle_{\text{nuc}}}{r^5} + \cdots\right\}, \tag{4}$$

where $\langle\cdots\rangle_{\text{nuc}}$ denotes a mean value taken over the nuclear charge density. When working to higher orders in $Z\alpha$ no such simple procedure is available. However, Eq. (4) provides a convenient check for our result. Solving the appropriate Dirac equation to order $Z\alpha$ we find, generally,

$$G/F = \frac{1}{2}Z\alpha\left(1 - \frac{\langle r^2\rangle_{\text{nuc}}}{3b^2}\right). \tag{5}$$

Substituting Eq. (5) into Eq. (3) and expanding we recover, as we must, the simple modification of the Uehling potential given by the first term in Eq. (4). The next two terms in Eq. (4) correspond to terms we neglect, terms involving more powers of $m_e a_\mu$ or b/a_μ. Since these dimensionless quantities are of the order of 0.1 to 0.2, we anticipate an accuracy satisfactory for the small effect being calculated.

The form of Eq. (3) may be understood as follows. Only b and r have dimensions since we

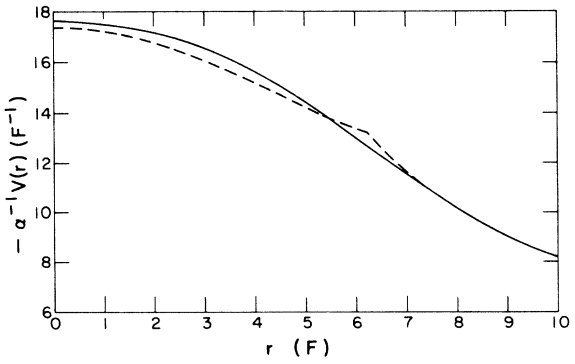

FIG. 2. A comparison of the model potential (dashed line) $V = A(r^2+a^2)^{-1/2}$ $(r<b)$, $V = -Z\alpha/r$ $(r>b)$, [Eq. (2)], with the electrostatic potential for Pb derived from its experimental charge distribution [J. Heisenberg *et al.*, Phys. Rev. Lett. 23, 1402 (1969)].

have set $m_e = 0$. Thus $\delta V(r)$ is given by r^{-1} times a function of the dimensionless ratio b/r. The ratio b/r appears to the power 2λ as a consequence of the well-known singular behavior of the Dirac wave function of lowest angular momentum at the origin of a Coulomb field. The factor in square brackets represents the effect of the $j = \frac{1}{2}$ phase shift caused by the non-point-like nuclear charge. Higher partial waves contribute with greater powers of b/r.

The energy shift of a muonic state due to the potential in Eq. (2) may be calculated by finding its expectation value for a Dirac wave function. Typical results are shown in Table I. We have calculated G/F for the model potential, Eq. (2), described in detail in Sec. III. Also displayed in Table I are the contributions from the finite-size corrections to the Uehling term, Eq. (4). In all these cases, the first term in Eq. (4) dominates, supporting our expectations for the higher-order terms in $Z\alpha$ that only the $m_e = 0$ term with the lowest power of b/r need be retained.

Focusing on ^{208}Pb, we see that finite nuclear size effects lower the $4f_{7/2}$ state by 20 eV and the $5g_{9/2}$ state by 6 eV. The Uehling piece accounts for 12 eV and 3 eV, respectively. Thus the $\alpha(Z\alpha)^n$, $n = 3, 5, 7\ldots$ terms of the finite-size effect increase the x-ray energy by 8 eV -3 eV $= 5$ eV. The resulting discrepancy is E(theory) $- E$(expt.) $= 54 \pm 17$ eV for this transition. Similar discrepancies exist for other high-Z atoms.[6]

These results are in agreement with the work of Arafune[8] and of Gyulassy.[10] Arafune's calculation was done only to order $\alpha(Z\alpha)^3$ and used the $m_e = 0$ approximation. The second term in an expansion in b/r was retained, and the calculation was done analytically for a model spherical nucleus with uniform charge density. Our result, Eq. (3), can be compared with Arafune's lower term in b/r by solving for G/F with his model nucleus and expanding to order $\alpha(Z\alpha)^3$ only. Our answer agrees precisely with his. Gyulassy calculates numerically the finite-size effect on the $j = \frac{1}{2}$ partial wave of the vacuum polarization. He keeps the electron mass finite, although his studies indicate it could safely be set to zero. He obtains excellent agreement with our analytical result.

The procedure followed in our calculation is straightforward, although technically complex. The vacuum-polarization charge density is given by the electron's Green's function with common space-time coordinates. For the point-source case, this is done in the conventional fashion of multiplying regular and irregular solutions to the radial Dirac equation for the Coulomb potential, as described in (I). A similar procedure may be followed for the nonpoint-source case. The solution which is regular at the origin, when evaluated outside the nucleus, must be a linear combination of the regular and irregular solutions to the pure Coulombic case since it satisfies the same homogeneous equation. The required linear combination is determined by G/F, which characterizes the regular solution to the true potential, evaluated at the nuclear surface. The result of this procedure is that the regular solution outside the nucleus has an admixture of the irregular solution to the point problem. On the other hand, the other function, which is bounded at infinity, evaluated outside the nucleus is the same for the finite nucleus and the point-nucleus cases. The difference between the Green's functions for the finite size and point-nuclear cases is then the product of two irregular solutions to the point case. The equal-time Green's function can be represented explicitly as an infinite integral in the complex-energy plane, along a contour which we choose to be the imaginary axis. The integral may be evaluated in closed form if we set $m_e = 0$.

The plan of this paper is as follows. In Sec. II we calculate the change in the vacuum-polariza-

TABLE I. Finite-size corrections to vacuum-polarization shifts of atomic energy levels in eV. The values of the parameters a and b [Eq. (2)] which were used were Ca, $a = 3.7$ F, $b = 4.1$ F; Ba, $a = 6.0$ F; $b = 5.6$ F; Pb, $a = 7.3$ F, $b = 6.3$ F.

		order $\alpha(Z\alpha)^n$, $n = 1, 3, 5, \ldots$	order $\alpha(Z\alpha)$ only		
		$m_e = 0$, lowest order in b/a_μ	$m_e = 0$, lowest in b/a_μ	$m_e \neq 0$ correction	higher order in b/a_μ
$^{40}Ca_{20}$	$3d_{5/2}$	−0.11	−0.10	0.02	0.00
	$4f_{7/2}$	−0.02	−0.02	0.01	0.00
$^{136}Ba_{56}$	$3d_{5/2}$	−15.9	−13.2	0.24	−0.35
	$4f_{7/2}$	−2.7	−2.0	0.14	−0.01
	$5g_{9/2}$	−0.7	−0.5	0.09	0.00
$^{208}Pb_{82}$	$3d_{5/2}$	−104	−83	0.69	−6.48
	$4f_{7/2}$	−20	−12	0.38	−0.15
	$5g_{9/2}$	−6	−3	0.25	−0.01

tion charge density arising from the finite nuclear size, in terms of a quantity depending on the nuclear charge distribution. The role of the nuclear charge distribution is discussed in Sec. III. The numerical results are given in Sec. IV. In Sec. V the various theoretical perturbations on muonic energy levels are discussed. The last section summarizes the work. An integral is evaluated in the Appendix.

II. THE VACUUM-POLARIZATION CHARGE DENSITY

The vacuum-polarization charge density is determined by the electron's Green's function for common space-time points. As discussed in (I), this relation may be expressed as an integral over the energy-dependent Green's function, Eq. (I.85):

$$\rho^F_{\text{vac pol}}(r) = -ie\int_{-i\infty}^{i\infty}\frac{dE}{2\pi}\,\text{tr}\,G^F(\vec{r},\vec{r};E)\gamma^0\,. \tag{6}$$

Here we write G^F to denote the true Green's function for the finite nucleus; G^C will denote the Green's function for the pure Coulomb (point-nucleus) case. The integration contour in Eq. (6) is along the imaginary E axis. The inhomogeneous equation satisfied by G^F is

$$\left[\vec{\gamma}\cdot\frac{1}{i}\vec{\nabla} - \gamma^0(E - V(r)) + m\right]G^F(\vec{r},\vec{r}';E) = \delta(\vec{r}-\vec{r}')\,, \tag{7}$$

where $V(r)$ is the potential energy of a negative charge in the actual electrostatic field of the nucleus, which we shall assume always to be spherically symmetric. The Coulomb-Dirac Green's function, G^C, satisfies this equation with $V(r) = -Z\alpha/r$. Outside the nucleus, the potential is purely Coulombic. Thus if r and r' are greater than the nuclear radius, b,

$$G^F(\vec{r},\vec{r}';E) = G^C(\vec{r},\vec{r}';E) + \delta G(\vec{r},\vec{r}';E)\,, \tag{8}$$

in which δG is a solution to the homogeneous counterpart of Eq. (7) with a point Coulomb potential.

The point Coulomb Green's function was constructed in paper I [Eq. (I.64)] in terms of an angular momentum expansion,

$$\begin{aligned} r>r':\quad & G^C(\vec{r},\vec{r}';E) = \sum_{K'}\sum_{m}\left(-\frac{\lambda}{q}\frac{K'}{k}\right)\frac{1}{r}\,\psi^m_{K'}(\vec{r};E)\bar{\phi}^m_{K'}(\vec{r}';E)\frac{1}{r'}\,,\\ r<r':\quad & G^C(\vec{r},\vec{r}';E) = \sum_{K'}\sum_{m}\left(-\frac{\lambda}{q}\frac{K'}{k}\right)\frac{1}{r}\,\phi^m_{K'}(\vec{r};E)\bar{\psi}^m_{K'}(\vec{r}';E)\frac{1}{r'}\,. \end{aligned} \tag{9}$$

Here the sums run over the Dirac quantum number $K' = \pm k = \pm(j+\frac{1}{2})$ and the magnetic quantum number m. The parameter $\lambda = [k^2 - (Z\alpha)^2]^{1/2}$, and $q = (m_e{}^2 - E^2)^{1/2}$ is real and positive along the imaginary energy axis. The spinor functions ϕ and ψ are regular at the origin and infinity, respectively. The Green's function for a finite nucleus, G^F, can be expanded in an entirely similar fashion. When both of its coordinates $(\vec{r},\vec{r}')$ lie outside the nuclear surface, the solution regular at infinity is the unique function ψ. However, the solution regular at the origin becomes a linear combination, $r>b$:

$${}^{(F)}\phi^m_{K'}(\vec{r};E) = \phi^m_{K'}(\vec{r};E) + R_{K'}(E)\psi^m_{K'}(\vec{r};E)\,. \tag{10}$$

The coefficient of the ϕ function which appears here must be unity so that the discontinuity at $\vec{r}=\vec{r}'$ [cf. Eq. (9)] produces the inhomogeneous δ function in the Green's function equation (7) with a coefficient of unity. The coefficient $R_{K'}(E)$ is determined by the condition that the function ${}^{(F)}\phi$ be continuous across the nuclear surface into the region where the potential is no longer Coulombic. In view of Eqs. (6), (8), (9), and (10), we see that outside the nuclear surface,

$$r>b:\quad \rho^F_{\text{vac pol}}(r) = \rho^C_{\text{vac pol}}(r) + \delta\rho(r)\,, \tag{11}$$

where $\rho^C_{\text{vac pol}}(r)$ is the vacuum-polarization charge induced by a point nucleus, and $\delta\rho(r)$ is the finite-size correction,

$$\delta\rho(r) = -ie\int_{-i\infty}^{i\infty}\frac{dE}{2\pi}\sum_{K'}\sum_{m}\left(-\frac{\lambda}{q}\frac{K'}{k}\right)R_{K'}(E) \times\frac{1}{r^2}\,\bar{\psi}^m_{K'}(\vec{r};E)\gamma^0\psi^m_{K'}(\vec{r};E)\,. \tag{12}$$

As explained in Sec. I, we shall compute $\delta\rho(r)$ to lowest order in b/r. Thus, we need retain only the lowest partial waves, $K' = \pm 1$, and we can take the electron mass to vanish, $m_e = 0$. The Green's function is chirally invariant when the electron mass vanishes: $G^{-1}\gamma^0$ commutes with γ_5. Since the Dirac operator $K = \gamma^0(\vec{\sigma}\cdot\vec{L}+1)$ anticommutes with γ_5, we conclude that terms with the two eigenvalues of this operator $K' = \pm k$ give identical contribution to Eq. (12) in the massless limit. We write $E = i\epsilon(= iq)$ and note that the lower portion of the integration $\epsilon < 0$ is the same as the complex

conjugation of the upper portion $\epsilon > 0$. Thus, the leading contribution to the finite size correction may be written as

$$\delta\rho_1(r) = -\frac{2e\lambda}{\pi}\,\mathrm{Re}\int_0^\infty \frac{d\epsilon}{\epsilon} R_1(i\epsilon) \times \sum_m \frac{1}{r^2}\,\bar{\psi}_1^m(\vec{r};i\epsilon)\gamma^0\psi_1^m(\vec{r};i\epsilon), \tag{13}$$

with now $\lambda = \lambda_1 = [1-(Z\alpha)^2]^{1/2}$.

The spinor functions that appear there were constructed in paper I [Eq. (I.58)]. With the electron mass vanishing, we have

$$\psi_1^m(\vec{r};i\epsilon) = i\left[\gamma^0\epsilon + \gamma_r\left(\frac{\partial}{\partial r} - \frac{\lambda}{r}\right)\right] \times A_{-\lambda}(r;i\epsilon)\chi^m_{1,-\lambda}(\hat{r}), \tag{14}$$

where $\gamma_r = \vec{\gamma}\cdot\hat{r}$, and $A_{-\lambda}$ is proportional to the Whittaker function regular at infinity. The spinor $\chi^m_{1,-\lambda}(\hat{r})$ is an eigenfunction of J_z and K with eigenvalues m and 1, respectively. It is also an eigenfunction of the operator $\mathcal{L} = -K\gamma^0 + iZ\alpha\gamma_r\gamma^0$ with eigenvalue $-\lambda$. Using the properties of these spinors listed in paper I [Eqs. (I.46) to (I.49)], and noting that, since the sum over magnetic quantum numbers is spherically symmetric we can average over solid angle, we compute

$$\delta\rho_1(r) = -\frac{e}{\pi^2 r^2}\,\mathrm{Re}\int_0^\infty \frac{d\epsilon}{\epsilon} R_1(i\epsilon)\left\{-\epsilon^2 A_{-\lambda}(r;i\epsilon)^2 + \left[\left(\frac{d}{dr} - \frac{\lambda}{r}\right)A_{-\lambda}(r;i\epsilon)\right]^2\right\}. \tag{15}$$

The joining coefficient $R_1(i\epsilon)$ is determined by the continuity of the wave function (10) at the nuclear surface, $r = b$. Since we are working only to leading order in b, we can use the short-distance limits of the spinor functions ϕ and ψ [Eqs. (I.42a), (I.42b), (I.60), (I.61)] to write the joining formula as

$$r = b:\ {}^{(F)}\phi_1^m(\vec{r};i\epsilon) = -\frac{(2\epsilon b)^\lambda}{\Gamma(2\lambda+1)}\,\chi^m_{1,-\lambda}(\hat{r}) + R_1(i\epsilon)\Gamma(2\lambda)(2\epsilon b)^{-\lambda}(2\epsilon)\chi^m_{1,\lambda}(\hat{r}). \tag{16}$$

We set

$$R_1(i\epsilon) = -\frac{(2\epsilon b)^{2\lambda}}{4\lambda\epsilon[\Gamma(2\lambda)]^2}\,H \tag{17}$$

to put the joining formula in the form

$$r = b:\ {}^{(F)}\phi_1^m(\vec{r};i\epsilon) = -\frac{(2\epsilon b)^\lambda}{\Gamma(2\lambda+1)}\left[\chi^m_{1,-\lambda}(\hat{r}) + H\chi^m_{1,\lambda}(\hat{r})\right]. \tag{18}$$

Now, with the electron mass vanishing, the functions in the integral (15) depend only upon the dimensionless variable $x = 2\epsilon r$,

$$A_{-\lambda}(r;i\epsilon) = \Gamma(\lambda - iZ\alpha)W_{iZ\alpha,\,\lambda-1/2}(x), \tag{19}$$

[Eq. (I.35)], where W is the Whittaker function that is regular at infinity. We can use x as the integration variable. Then the energy dependence of the joining coefficient appears through $2\epsilon = x/r$. Hence, the leading power of b/r involves the $\epsilon \to 0$ limit of the joining formula (18), where H becomes a dimensionless constant depending only upon the nuclear shape. [The overall factor of $(2\epsilon b)^\lambda$ in Eq. (18) is irrelevant. We are concerned here only with the relative weights of the spinors $\chi^m_{1,\pm\lambda}$ in ${}^{(F)}\phi_1^m$.] Accordingly,

$$\delta\rho_1(r) = \frac{e}{\pi^2}\frac{1}{r^3}\left(\frac{b}{r}\right)^{2\lambda}\frac{H}{2\lambda\Gamma(2\lambda)^2}\,\mathrm{Re}\int_0^\infty dx\,x^{2\lambda}\left\{-\tfrac{1}{4}W_{iZ\alpha,\lambda-1/2}(x)^2 + \left[\left(\frac{d}{dx} - \frac{\lambda}{x}\right)W_{iZ\alpha,\lambda-1/2}(x)\right]^2\right\}\Gamma(\lambda - iZ\alpha)^2. \tag{20}$$

This integral is evaluated in the Appendix. Using that result and solving Poisson's equation for the potential energy, we secure

$$\delta V(r) = \frac{4\alpha}{\pi r}\left(\frac{b}{r}\right)^{2\lambda} H\frac{\Gamma(4\lambda)}{(2\lambda)^2(2\lambda+1)^2}\left|\frac{\Gamma(\lambda+iZ\alpha)}{\Gamma(2\lambda)}\right|^4. \tag{21}$$

There remains the computation of the dimensionless joining coefficient H. It is determined by the formula (18) with ${}^{(F)}\phi_1^m(\vec{r};i\epsilon)$ the regular solution to the Dirac equation within the nuclear surface evaluated at zero energy and zero mass. We shall develop this equation in the usual spinor basis provided by $\chi^{l,m}_\pm$, which are eigenfunctions of K and J_z with eigenvalues 1 and m, respectively. These spinors also diagonalize γ^0,

$$\gamma^0\chi^{l,m}_\pm = \pm\chi^{l,m}_\pm. \tag{22}$$

Since γ_r anticommutes with γ^0 and squares to -1, we set

$$\gamma_r \chi^{1,m}_{\pm} = i\chi^{1,m}_{\mp} . \tag{23}$$

We write

$$^{(F)}\phi^m_1(\vec{r};0) = \frac{1}{r}\left[F(r)\chi^{1,m}_{+}(\hat{r}) + G(r)\chi^{1,m}_{-}(\hat{r})\right], \tag{24}$$

and use [Eq. (I.15)]

$$\vec{\gamma}\cdot\frac{1}{i}\vec{\nabla} = \gamma_r \frac{1}{i}\left(\frac{\partial}{\partial r} + \frac{1}{r}\right) - \frac{i\gamma^0\gamma_r K}{r} \tag{25}$$

to express the Dirac equation [Eq. (7) in homogeneous form with $E = m = 0$] as the coupled equations

$$\left[\frac{d}{dr} + \frac{1}{r}\right] G(r) = -V(r)F(r) , \tag{26a}$$

$$\left[\frac{d}{dr} - \frac{1}{r}\right] F(r) = V(r)G(r) . \tag{26b}$$

We shall solve these equations for a model potential, Eq. (2), in the following section. We conclude this section by solving the general relationship among F, G, and H for an arbitrary potential $V(r)$,

$$F(b)\chi^{1,m}_{+} + G(b)\chi^{1,m}_{-} = (\text{const})[\chi^m_{1,-\lambda} + H\chi^m_{1,\lambda}] . \tag{27}$$

This is accomplished by relating the two spinor bases. We consider the action of γ^0 and γ_r both to the right and to the left in $\bar{\chi}^m_{1,\lambda}\gamma^0\chi^{1,m}_{\pm}$ and $\bar{\chi}^m_{1,\lambda}\gamma_r\chi^{1,m}_{\pm}$ using Eqs. (22), (23), and Eqs. (I.46), (I.48). These equations imply the relations

$$\bar{\chi}^m_{1,\lambda}\chi^{1,m}_{+}(\lambda+1) = Z\alpha\bar{\chi}^m_{1,-\lambda}\chi^{1,m}_{+} , \tag{28a}$$

$$\bar{\chi}^m_{1,\lambda}\chi^{1,m}_{-} = -\bar{\chi}^m_{1,-\lambda}\chi^{1,m}_{+} , \tag{28b}$$

$$\bar{\chi}^m_{1,\lambda}\chi^{1,m}_{+} = \bar{\chi}^m_{1,-\lambda}\chi^{1,m}_{-} , \tag{28c}$$

which, together with the orthonormality relations between the $\chi^m_{1,\pm\lambda}$ [Eq. (I.49)], yield

$$H = H(b) = -\frac{[Z\alpha/(1+\lambda)]F(b) - G(b)}{F(b) - [Z\alpha/(1+\lambda)]G(b)} . \tag{29}$$

Inserting this into Eq. (21) gives the result (3) quoted in the Introduction.

III. ROLE OF THE NUCLEAR CHARGE DENSITY

The expression for the change in the vacuum-polarization potential energy due to the finite nuclear size, Eq. (3), depends on the nuclear charge density through the quantity $b^{2\lambda}H(b)$. It must be the same whether evaluated at the edge of the charge distribution or somewhere outside it. The coupled Dirac equations, Eq. (26), yield a differential equation

$$\frac{d}{db}\left[b^{2\lambda}H(b)\right] = \left[-\frac{Z\alpha}{b} - V(b)\right]\left[1 + 2Z\alpha H(b) + H^2(b)\right]/\lambda . \tag{30}$$

Outside the nuclear charge distribution $V(b) = -Z\alpha/b$ and $b^{2\lambda}H(b)$ is indeed constant. Equation (30) is nonlinear (a Ricatti equation), and we cannot solve it directly. However, given $V(b)$ (or equivalently, the nuclear charge distribution) it can be solved numerically to determine H (b = nuclear radius). The lowest-order result in $Z\alpha$ can be obtained from Eq. (30) in the form

$$\frac{d(b^2H^1)}{db} = b^2\left[-\frac{Z\alpha}{b} - V(b)\right] . \tag{31}$$

This can be integrated with the result

$$H^1(b) = -\frac{Z\alpha}{6}\frac{\langle r^2\rangle_{\text{nuc}}}{b^2} , \tag{32}$$

where $\langle r^2\rangle_{\text{nuc}}$ is the mean squared radius of the nuclear charge. This gives for the potential-energy change

$$\delta V(r) = -\frac{\alpha Z\alpha}{9\pi r^3}\langle r^2\rangle_{\text{nuc}} , \tag{33}$$

in agreement with Eq. (4).

While the differential equation (30) can be used for any input potential, for our purposes it suffices to use a model potential,

$$V(r) = A(r^2 + a^2)^{-1/2} , \tag{2}$$

for r less than b, the nuclear radius. From the coupled Dirac equations, Eq. (26), we can form the second-order equation,

$$\left[\frac{d^2}{dr^2} - \frac{1}{V}\frac{dV}{dr}\left(\frac{d}{dr} - \frac{1}{r}\right) + V^2\right] F(r) = 0 . \tag{34}$$

With the model potential above, the equation has only regular singular points. In fact, with $r = a\sinh u$, we find

$$\left(\frac{d^2}{du^2} - 1 + A^2\right) F(u) = 0 , \tag{35}$$

which has the regular solution

$$F = C\sinh(1-A^2)^{1/2}u . \tag{36}$$

From Eq. (26b) we find then that

$$G = \frac{C}{A}\left[(1-A^2)^{1/2}\cosh(1-A^2)^{1/2}u - \coth u\sinh(1-A^2)^{1/2}u\right] . \tag{37}$$

The parameters of the potential are A, a, and b, the radius at which the potential becomes Coulombic. Thus we have the constraint

$$A/(a^2+b^2)^{1/2} = -Z\alpha/b . \tag{38}$$

The remaining parameters, a and b, can be chosen to reproduce approximately the electrostatic potential inside the nucleus. The nuclear charge distributions are only known approximately,[12] and our treatment is quite accurate enough, considering these uncertainties and the smallness of the effect itself.

IV. NUMERICAL RESULTS

Table I displays some numerical results for the level shifts resulting from the finite nuclear charge distribution effect on vacuum polarization. The values of the charge distribution parameters which have been used, a and b, are also given. A typical fit to the electrostatic potential is shown in Fig. 2. The finite nuclear size correction for the Uehling potential, Eq. (4), is displayed for comparison. We have calculated to all orders in $Z\alpha$ using $m_e = 0$ and keeping only the first term in b/a_μ. This corresponds to the first term in Eq. (4). The next two terms are corrections for $m_e \neq 0$ and higher-order terms in b/a_μ.

Table I reveals that it is necessary to go beyond the Uehling order only for very large Z, as in $^{208}_{82}$Pb. The $m_e = 0$ approximation seems very well justified on the basis of the Uehling term. Higher-order terms in b/a_μ are small except for the third level in ^{208}Pb. Even in this case, for the $\alpha(Z\alpha)^n$ terms with $n \geq 3$, the approximation is probably good to $\simeq 2$ eV. For the well-studied transition, $5g_{9/2} \rightarrow 4f_{7/2}$ in ^{208}Pb, we find the levels shifted down by 6 eV and 20 eV, respectively. The Uehling terms are responsible for 3 eV and 12 eV, respectively. Altogether, the x-ray transition energy is increased by 8 eV − 3 eV = 5 eV by the finite nuclear size correction to vacuum polarization in orders higher than $\alpha(Z\alpha)$.

Our result for ^{208}Pb is in agreement with the $k = 1$ numerical calculation of Gyulassy.[10] It also agrees with the $\alpha(Z\alpha)^3$ analytical calculation of Arafune.[8] The first calculation of the effect was a numerical computation by Rinker and Wilets.[7] Although they reported a 16 ± 2 eV rather than a 5 eV contribution for the finite-size correction with the Uehling term removed, more recent work by the same authors is in agreement with our results.[13]

V. REVIEW OF THEORETICAL CALCULATIONS OF ENERGY LEVELS

The various corrections which must be made to the Dirac energy levels have been described by Blomqvist[5] and Sundaresan and Watson.[6] In Table II we display the corrections for the transition $5g_{9/2} \rightarrow 4f_{7/2}$ in ^{208}Pb. Some of the potentials associated with these effects are displayed in Fig. 3.

TABLE II. Theoretical determination of the x-ray transition energy for $5g_{9/2} \rightarrow 4f_{7/2}$ in muonic ^{208}Pb. The values come from the present work, (I), (II), and Ref. 5. All numbers are in eV. The individual entries under "short distance" and "Electron screening" contain convenient but arbitrary constant potential pieces. Only the differences between the two columns for these figures, the transition energy contributions, are significant.

Contribution	$4f_{7/2}$	$5g_{9/2}$
Vacuum polarization:		
point nucleus		
$\alpha Z\alpha$	−3652	−1562
$\alpha(Z\alpha)^n$ $n = 3, 5, \ldots$		
induced point charge	+152	+97
short distance	+18	+26
2nd-order Uehling	−9	−3
$\alpha^2 Z\alpha$	−25	−11
finite-nucleus correction	−20	−6
Total vacuum polarization	−3536	−1459
Dirac (with reduced mass)	−1 188 316	−758 971
Finite nucleus	+4	0
Nuclear motion, relativity	−4	−2
Radiative effects (Lamb shift)	+10	+3
Electron screening	−77	−155
Nuclear polarization	−4	0
	−1 191 923	−760 584
$E_5 - E_4 = 431\,339$ eV		

Examination of Table II and Fig. 3 reveals that the Coulomb potential is predominant of course, and is of the order of MeV at the radii of these orbits (50–80 F, or $m_e r \simeq 0.15$–0.22). The Uehling potential is seen to be of the order of keV and increases the x-ray energy.

The induced point charge for Pb is ^{2,3} $-5.2 \times 10^{-3} e$. It gives a potential of Coulombic behavior, but of sign opposite that of the direct Coulomb potential. It thus decreases the x-ray transition energy. The $4f$ state is shifted by $\alpha(-\delta Q/e)\langle 1/r\rangle = +152$ eV, while the $5g$ is shifted by +97 eV.

Still treating the nucleus as a point charge, the induced vacuum-polarization charge density may be expanded in powers[4] of $m_e r$. Since the Uehling term has already been computed, terms of order $\alpha Z\alpha$ must not be included. In this way three potentials beyond the $\alpha Z\alpha$ approximation are obtained: (1) order $m(mr)$, (2) order $m(mr)^{2\lambda}$, (3) the difference between the $\alpha Z\alpha$ piece of the $m(mr)^{2\lambda}$ potential and its $\alpha Z\alpha$ approximation which is of order $m(mr)^2$. As explained in (II) these potentials are of a significant size, about 50 eV for the $m(mr)$ potential. As indicated in Table II, their cumulative effect is only 8 eV. Moreover, substantial cancellations occur among terms of order

higher than $\alpha(Z\alpha)^3$, so that they account for only 1 eV of this 8 eV.

The potential associated with the finite nuclear size effect on vacuum polarization has a very different r dependence. The $m(mr)^{-2\lambda-1}$ potential decreases very quickly as r increases. In fact, our calculation is applicable only for r much greater than the nuclear radius, which for Pb is about 7 F, or $mr \simeq 0.02$. The $4f$ state has its energy decreased by 20 eV and the $5g$ state is lowered by 6 eV. These figures include the finite-size corrections to the Uehling term.

To the above-mentioned effects, we must add other vacuum-polarization effects which have been calculated by other authors. These have been compiled by Blomqvist.[5] The first is the contribution of the Uehling potential in second-order perturbation. This then is an effect of order $(\alpha Z\alpha)^2$. Another is the vacuum polarization of order $\alpha^2 Z\alpha$. Its contribution also has been calculated by Blomqvist.[5] A further correction related to vacuum polarization is the term of order $\alpha^2(Z\alpha)^2$ in which there is a single electron loop with two attachments from the muon and two from the nucleus. The contribution of this diagram is still the subject of controversy,[14,15] and we have not included it in our tabulation.

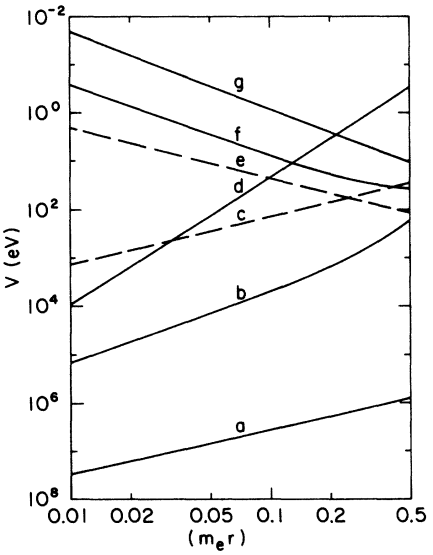

FIG. 3. Contributions to the potential energy of a μ^- in the electrostatic field about a ^{208}Pb nucleus as a function of radius. (a) The Coulomb energy, (b) the Uehling energy, (c) induced point charge contribution, (d) finite nuclear size corrections to vacuum polarization, (e) $m(mr)$ term of vacuum polarization with Uehling term removed, (f) $\alpha Z\alpha$ term of $m(mr)^{2\lambda}$ potential minus its Uehling approximation, (g) $m(mr)^{2\lambda}$ term with the $\alpha Z\alpha$ piece removed. Solid lines indicate negative potential energy, dashed lines positive potential energy.

The remaining corrections are not directly related to vacuum polarization. These include the finite nuclear size effect directly on the muon, corrections to the static-nucleus approximation, radiative effects (Lamb shift), electron screening,[16] and nuclear polarization. We shall use the values cited by Blomqvist[5] for these corrections in Table II.

The most recent experiment is that of Dixit *et al.*,[17] who find an energy of 431 285 eV ± 17 eV. The theoretical number itself has uncertainties. The simplest of these is the uncertainty in the muon mass and squared fine-structure constant which scale the Dirac energy. The uncertainty in the muon mass is about 3 parts per million, and the uncertainty in α^2 is about 2 parts per million. These introduce an uncertainty of 1 eV in the transition energy. The more serious uncertainties arise from neglecting contributions such as the single-loop diagram of order $\alpha^2(Z\alpha)^2$. In addition, contributions could arise from less conventional sources. These might include hitherto unobserved particles[18] and/or nonperturbative effects.[19]

Except for the $\alpha^2(Z\alpha)^2$ term, the vacuum-polarization corrections seem no longer to be controversial. Our results are in good agreement with those of Gyulassy,[10] whose computer studies eliminate the need to expand in mr. Gyulassy calculates only the $k = j + \frac{1}{2} = 1$ partial waves, and then makes a small correction to approximate the higher partial waves.

VI. SUMMARY

This paper concludes our three-part study of vacuum polarization in the strong Coulomb field surrounding a nucleus. Throughout, we have calculated to all orders in $Z\alpha$, as is appropriate to high-Z atoms such as ^{208}Pb. In the first paper techniques for using the massless electron approximation for the Dirac-Coulomb Green's function were presented and used to evaluate the induced point charge. In the second paper the general form of the induced vacuum-polarization charge density was obtained. The first two papers provide a complete treatment of vacuum polarization around a point nucleus, to first order in α and all orders in $Z\alpha$.

In this paper we have accounted for the change in the vacuum polarization resulting from the finite extent of the nuclear charge distribution. As in the two preceding papers, all calculations were done analytically, and to all orders in $Z\alpha$.

We have applied our calculations to the determination of muonic x-ray transitions. These provide critical tests of quantum electrodynamics.

Even after all known effects are taken into account, discrepancies persist, especially in the well-studied transition, $5g_{9/2} - 4f_{7/2}$ in ^{208}Pb, where we find $E_{\rm th} - E_{\rm exp} = 54\ {\rm eV} \pm 17\ {\rm eV}$.

Note added in proof. The single-electron-loop graphs involving two-photon exchange with both the muon and the nucleus, which are of order $\alpha^2(Z\alpha)^2$, have been calculated recently by Fujimoto.[22] He makes the plausible approximations of a static muon and massless virtual electrons. Using a Monte Carlo integration method, Fujimoto finds an energy shift of 0.76(3) eV for the $5g_{9/2} - 4f_{7/2}$ transition in ^{208}Pb.

ACKNOWLEDGMENTS

We wish to thank our colleague, L. Wilets, for bringing this problem to our attention and for discussions of the physics of the problem. We would also like to thank S. J. Brodsky, M. Gyulassy, P. Mohr, and E. Wichmann for useful discussions.

APPENDIX

Equation (20) involves the integral

$$I = \mathrm{Re} \int_0^\infty dx\, x^{2\lambda} \left\{ -\tfrac{1}{4} W_{i\zeta,\lambda-1/2}(x)^2 + \left[\left(\frac{d}{dx} - \frac{\lambda}{x} \right) W_{i\zeta,\lambda-1/2}(x) \right]^2 \right\} \Gamma(\lambda - i\zeta)^2 , \tag{A1}$$

where $\zeta = Z\alpha$. Using the differential equation

$$\left[\frac{d^2}{dx^2} - \frac{1}{4} + \frac{i\zeta}{x} - \frac{\lambda(\lambda-1)}{x^2} \right] W_{i\zeta,\lambda-1/2}(x) = 0 , \tag{A2}$$

integrations by parts yield the equivalent form

$$I = \mathrm{Re} \int_0^\infty dx\, x^{2\lambda-2} W_{i\zeta,\lambda-1/2}(x)^2 [4\lambda^2 - \lambda + i\zeta x - \tfrac{1}{2}x^2]\, \Gamma(\lambda - i\zeta)^2 . \tag{A3}$$

We define

$$J_p = \int_0^\infty dx\, x^{2\lambda-p} W_{i\zeta,\lambda-1/2}(x)^2 \Gamma(\lambda - i\zeta)^2 , \tag{A4}$$

which is needed for $p = 0, 1, 2$. We represent one Whittaker function by

$$W_{i\zeta,\lambda-1/2}(x) = \frac{x^\lambda e^{-x/2}}{\Gamma(\lambda - i\zeta)} \int_0^\infty dt\, e^{-xt} (1+t)^{i\zeta+\lambda-1} t^{-i\zeta+\lambda-1} , \tag{A5}$$

and use the integral[20]

$$\int_0^\infty dx\, x^{3\lambda-p} e^{-x(t+1/2)} W_{i\zeta,\lambda-1/2}(x) = \frac{\Gamma(4\lambda-p+1)\Gamma(2\lambda-p+2)}{\Gamma(3\lambda-p-i\zeta+2)} (t+1)^{-3\lambda+p-1} \times F\left(4\lambda-p+1, \lambda-i\zeta; 3\lambda-p-i\zeta+2; \frac{t}{t+1}\right), \tag{A6}$$

where $F(a, b; c; z)$ is the usual hypergeometric function. It obeys

$$F(a, b; c; z) = (1-z)^{c-a-b} F(c-b, c-a; c; z) . \tag{A7}$$

Inserting Eq. (A5) into Eq. (A4), using the integral (A6), the relation (A7), and changing variables to $\tau = t(1+t)^{-1}$, we secure

$$J_p = \frac{\Gamma(4\lambda+1-p)\Gamma(2\lambda+2-p)\Gamma(\lambda-i\zeta)}{\Gamma(3\lambda+2-p-i\zeta)} \int_0^1 d\tau\, \tau^{-i\zeta+\lambda-1} (1-\tau)^{2-p} F(2\lambda+2-p, 1-\lambda-i\zeta; 3\lambda+2-p-i\zeta; \tau) . \tag{A8}$$

The following formula[21] enables us to complete the calculation:

$$\frac{\Gamma(2\lambda+2-s)}{\Gamma(\lambda+i\zeta)\Gamma(3\lambda+2-s-i\zeta)}\int_0^1 d\tau\,\tau^{\lambda-(1/2)s-\nu}F(2\lambda+2-s,1-\lambda-i\zeta;3\lambda+2-s-i\zeta;\tau)$$
$$+\frac{\Gamma(2\lambda+2-s)}{\Gamma(\lambda-i\zeta)\Gamma(3\lambda+2-s+i\zeta)}\int_0^1 d\tau\,\tau^{\lambda-(1/2)s+\nu}F(2\lambda+2-s,1-\lambda+i\zeta;3\lambda+2-s+i\zeta;\tau)$$
$$=\frac{\Gamma(\lambda+1-\frac{1}{2}s+\nu)\Gamma(\lambda+1-\frac{1}{2}s-\nu)}{\Gamma(2\lambda+1-\frac{1}{2}s-i\zeta+\nu)\Gamma(2\lambda+1-\frac{1}{2}s+i\zeta-\nu)}\,. \quad \text{(A9)}$$

First, we set $\nu=i\zeta$ to obtain

$$2\,\mathrm{Re}\,\frac{\Gamma(2\lambda+2-s)}{\Gamma(\lambda+i\zeta)\Gamma(3\lambda+2-s-i\zeta)}\int_0^1 d\tau\,\tau^{\lambda-(1/2)s-i\zeta}F(2\lambda+2-s,1-\lambda-i\zeta;3\lambda+2-s-i\zeta;\tau)=\left|\frac{\Gamma(\lambda+1-\frac{1}{2}s+i\zeta)}{\Gamma(2\lambda+1-\frac{1}{2}s}\right|^2. \quad \text{(A10)}$$

Specializing Eq. (A10) to $s=2$ gives directly

$$\mathrm{Re}J_2=\frac{\Gamma(4\lambda-1)|\Gamma(\lambda-i\zeta)|^4}{2\Gamma(2\lambda)^2}\,. \quad \text{(A11)}$$

Specializing Eq. (A10) to $s=0$ gives one piece of $\mathrm{Re}J_0$ [that involving the cross term -2τ in $(1-\tau)^2$]. Next, we set $s=0$ in Eq. (A9) and add the formulas for $\nu=i\zeta+1$ and $\nu=i\zeta-1$ to obtain

$$\mathrm{Re}\,\frac{\Gamma(2\lambda+2)}{\Gamma(\lambda+i\zeta)\Gamma(3\lambda+2-i\zeta)}\int_0^1 d\tau\,\tau^{\lambda-1-i\zeta}(1+\tau^2)F(2\lambda+2,1-\lambda-i\zeta;3\lambda+2-i\zeta;\tau)=\mathrm{Re}\,\frac{\Gamma(\lambda-i\zeta)\Gamma(\lambda+2+i\zeta)}{\Gamma(2\lambda)\Gamma(2\lambda+2)}\,, \quad \text{(A12)}$$

which gives the remaining pieces of $\mathrm{Re}J_0$. Thus,

$$\mathrm{Re}J_0=\frac{\Gamma(4\lambda+1)|\Gamma(\lambda-i\zeta)|^4}{2\lambda\Gamma(2\lambda)^2}\left[\frac{2\lambda^2+\lambda-1}{2\lambda+1}-\frac{1}{2\lambda}\right]. \quad \text{(A13)}$$

Finally, we set $s=1$ in Eq. (A9) and subtract the formula with $\nu=i\zeta-\frac{1}{2}$ from that with $\nu=i\zeta+\frac{1}{2}$ to derive

$$\mathrm{Im}J_1=\frac{\Gamma(4\lambda)|\Gamma(\lambda-i\zeta)|^4}{\Gamma(2\lambda)^2}\left[\frac{\zeta}{2\lambda}\right]. \quad \text{(A14)}$$

It is now a trivial matter to evaluate

$$I=(4\lambda-1)\lambda\,\mathrm{Re}J_2-\zeta\,\mathrm{Im}J_1-\tfrac{1}{2}\mathrm{Re}J_0=\frac{\Gamma(4\lambda)}{\Gamma(2\lambda)^2}\,\frac{|\Gamma(\lambda-i\zeta)|^4}{2\lambda+1}\,, \quad \text{(A15)}$$

giving Eq. (21).

---

*Research supported in part by the U. S. Atomic Energy Commission.

[1]E. A. Uehling, Phys. Rev. 48, 55 (1935).
[2]E. H. Wichmann and N. M. Kroll, Phys. Rev. 101, 843 (1956).
[3]L. S. Brown, R. N. Cahn, and L. D. McLerran, this issue, Phys. Rev. D 12, 581 (1975); hereafter called (I).
[4]L. S. Brown, R. N. Cahn, and L. D. McLerran, Phys. Rev. Lett. 33, 1591 (1974); preceding paper, Phys. Rev. D 12, 596 (1975), hereafter called (II).
[5]J. Blomqvist, Nucl. Phys. B48, 95 (1972). Table 2 of this reference contains a misprint. The third entry of the first column should be (−4) rather than (−8).
[6]P. J. S. Watson and M. K. Sundaresan, Can. J. Phys. 52, 2037 (1974).
[7]G. A. Rinker, Jr. and L. Wilets, Phys. Rev. Lett. 31, 1559 (1973).
[8]J. Arafune, Phys. Rev. Lett. 32, 560 (1974).
[9]L. S. Brown, R. N. Cahn, and L. D. McLerran, Phys. Rev. Lett. 32, 562 (1974).
[10]M. Gyulassy, Phys. Rev. Lett. 32, 1393 (1974).
[11]A. B. Mickelwait and H. C. Corben, Phys. Rev. 96, 1145 (1954).
[12]R. C. Barrett, Rep. Prog. Phys. 37, 1 (1974).
[13]L. Wilets (private communication).
[14]M. -Y. Chen, Phys. Rev. Lett. 34, 341 (1975).
[15]L. Wilets and G. A. Rinker, Jr., Phys. Rev. Lett. 34, 339 (1975).
[16]J. Blomqvist cites M. S. Dixit *et al.*, Phys. Rev. Lett. 27, 878 (1971), and H. L. Anderson, in *High-Energy Physics and Nuclear Structure*, Third International Conference held at Columbia University, New York, 1969, edited by S. Devons (Plenum, New York, 1970), p. 640. B. Fricke [Nuovo Cimento Lett. 11, 859 (1969)] and P. Vogel [Phys. Rev. A 7, 63 (1973)] have also calculated the electron screening contribution. For the $5g\rightarrow 4f$ transition in Pb, Dixit *et al.* find that the effect decreases the x-ray energy by 78 eV [cf. Table II]. Fricke finds 80 eV, while Vogel finds 83 eV.

[17]M. S. Dixit *et al.*, Phys. Rev. Lett. 27, 878 (1971). An earlier experiment, G. Backenstoss *et al.*, Phys. Lett. 31B, 233 (1970), obtained 431 410 ± 40 eV.
[18]L. Resnick, M. K. Sundaresan, and P. J. S. Watson, Phys. Rev. D 8, 172 (1973); S. Adler, R. Dashen, and S. B. Treiman, *ibid.* 10, 3728 (1974).
[19]S. L. Adler, Phys. Rev. D 10, 3714 (1974). New results on the muon $g-2$, J. Bailey *et al.*, Phys. Lett. 55B, 420 (1975), seem to rule out this proposal of Adler.
[20]I. S. Gradshteyn and I. M. Ryzhik, *Tables of Integrals, Series and Products* (Academic, New York, 1965), p. 860.
[21]*Higher Transcendental Functions* (Bateman Manuscript Project), edited by A. Erdélyi (McGraw-Hill, New York, 1953), Vol. 1, p. 79, Eq. (5).
[22]D. H. Fujimoto, Univ. of Washington report (unpublished).